

DISCLAIMER

Conf-9409178-8

This report was prepared as an account of work sponsored by an agency of the United States Government. Neither the United States Government nor any agency thereof, nor any of their employees, makes any warranty, express or implied, or assumes any legal liability or responsibility for the accuracy, completeness, or usefulness of any information, apparatus, product, or process disclosed, or represents that its use would not infringe privately owned rights. Reference herein to any specific commercial product, process, or service by trade name, trademark, manufacturer, or otherwise does not necessarily constitute or imply its endorsement, recommendation, or favoring by the United States Government or any agency thereof. The views and opinions of authors expressed herein do not necessarily state or reflect those of the United States Government or any agency thereof.

COMPARISON OF GLASSY SLAG WASTE FORMS PRODUCED IN LABORATORY CRUCIBLES AND IN A BENCH-SCALE PLASMA FURNACE

X. Feng, D. J. Wronkiewicz, N. R. Brown, and M. Gong

ARGONNE NATIONAL LABORATORY
Chemical Technology Division
9700 South Cass Avenue
Argonne, IL 60439-4837

and

C. Whitworth, K. Filius, and D. Battleson

MSE, INC.
P. O. Box 3767
Butte, MT 59702

The submitted manuscript has been authored by a contractor of the U. S. Government under contract No. W-31-109-ENG-38. Accordingly, the U. S. Government retains a nonexclusive, royalty-free license to publish or reproduce the published form of this contribution, or allow others to do so, for U. S. Government purposes.

Accepted for Presentation at
American Chemical Society Special Symposium
Emerging Technologies in Hazardous Waste Management VI
Atlanta, Georgia
September 19-21, 1994

This work is supported by the Office of Technology Development, within the U.S. Department of Energy's Office of Environmental Management, under Contract W-31-109-ENG-38 and DE-AC22-88ID12735.

MASTER

DISTRIBUTION OF THIS DOCUMENT IS UNLIMITED

g7D

DISCLAIMER

**Portions of this document may be illegible
in electronic image products. Images are
produced from the best available original
document.**

**Comparison of Glassy Slag Waste Forms Produced in Laboratory
Crucibles and in a Bench-Scale Plasma Furnace**

X. Feng, D. J. Wronkiewicz, N. R. Brown, and M. Gong
Chemical Technology Division
Argonne National Laboratory

and

C. Whitworth, K. Filius, and D. Battleson
MSE, Inc.

ABSTRACT

Glassy slags (vitro-ceramics) are glass-crystal composites, and they are composed of various metal oxide crystalline phases embedded in an aluminosilicate glass matrix. Glassy slags are developed to complement homogenous glass waste forms in implementing Minimum Additive Waste Stabilization (MAWS). Glassy slags with compositions developed in crucible melts at Argonne National Laboratory (ANL) were successfully produced in a bench-scale Retech plasma centrifugal furnace (PCF) by MSE, Inc. Detailed examinations of these materials showed that the crucible melts and the PCF produced similar glass and crystalline phases. The two sets of glassy slags exhibited similar chemical durability in terms of normalized releases of their major components. The slags produced in the PCF furnace using metals were usually less oxidized, although this had no effect on the corrosion behavior of the major components of the slags. However, the normalized release rate of cerium was initially lower for the PCF slags. This difference diminished with time as the redox states of the metal oxides in slags began to be controlled by exposure to air in the tests. Thus, the difference in cerium release due to the differences in slag redox state may be transitory. The cerium solubility is a complex function of redox state and solution pH and Eh.

INTRODUCTION

Vitrification is currently the best demonstrated available technology for the disposal of high-level nuclear wastes. An innovative vitrification approach known as minimum additive waste stabilization (MAWS) is being developed [1]. Both homogeneous glass and glassy slags have been used in implementing MAWS [2]. In the MAWS approach, the available waste streams are utilized as resources for the glass-making process, and multiple waste streams are blended to minimize the need for the purchased additives usually required for stabilization. The goal of the MAWS approach is to achieve maximum reduction in waste volume and maximum cost savings. Glassy slags (Vitro-Ceramics) are glass-crystal composites, and they are composed of various metal oxide crystalline phases embedded in an aluminosilicate glass matrix.

To develop final waste forms for high-metal-content waste streams, glassy slags have been produced by melting soils from Idaho National Engineering Laboratory (INEL) with metal oxides in crucibles. The melts simulate the treatment of waste streams that contain metals such as contaminated carbon steel and stainless steel scrap, tools, and equipment. This laboratory work was coordinated with work at MSE, Inc., where slags were prepared in a prototype plasma centrifugal furnace (PCF). This type of high-temperature vitrifier represents one potential means of treating wastes. Slags with metal oxide contents up to 84 wt % were prepared by melting the materials at 1500°C. Glassy slags have been shown to exhibit advantages of both glass waste forms and Synroc waste forms and can be made entirely from wastes [3-4].

To show that the formulations developed during the crucible melting at Argonne National Laboratory (ANL) are transferable to bench-scale production with a PCF, a total of eight formulations were recommended to MSE for test runs in a 1.5-ft PCF of Retech, Inc. This assessment includes the processibility and product properties. The processibility has been successfully demonstrated by MSE, and all the melts recommended were produced in the 1.5-ft Retech PCF in August 1993. The following discussion will focus on a comparison of the properties of the slags made in the crucible melts and in the Retech PCF.

EXPERIMENTAL

ANL Slag Preparation

Glassy slags were produced in crucibles by melting as-received INEL soil with metal oxides (such as Fe_2O_3 , Cr_2O_3 , and NiO) to simulate high-metal-content waste streams, such as those containing contaminated carbon steel and stainless steel scrap, tools, and equipment. Two slags were also made in which additional Al_2O_3 was used to simulate scrap aluminum metal. Three slags were made with PbO to determine how lead is partitioned in slags. One slag was made with SiO_2 to determine if sand can improve slag durability. (Some U.S. Department of Energy sites, such as the Oak Ridge site, have waste sands.) Twelve slags were made with CeO_2 , which served as a surrogate for plutonium. The formulations in terms of INEL soil and waste metals are shown in Table 1. The highest metal loading was 74 wt % (slag ANL-M2). Because the INEL soil we used contains 22 wt % volatile materials, the actual metal loading is 78 wt % in terms of dried INEL soil. This translates into a 84 wt % metal oxide loading (Table 2). All these melts contain zero additives, i.e., the waste loading is 100%, because all the feeds were surrogates for actual wastes.

A batch of about 300 g of the mixture of chemicals and INEL soil was ball milled for more than 4 h to ensure complete mixing. The mixture, contained in a high-alumina crucible (99.8% Al_2O_3), was then put into a furnace preheated to about 800°C. The temperature of the furnace was then quickly raised to 1500°C. The molten slag was kept at 1500°C for 40 min to 1 h. If the melt was pourable, it was quenched by pouring it into a platinum mold. The poured slag was annealed for 1 h at about 500°C; then the furnace was turned off to cool to room temperature. If the melt was not pourable, it was air cooled in the melt crucible.

Slag Production at MSE using 1.5-ft PCF

The 1.5-ft PCF is an engineering-scale remedial thermal technology process which uses the heat generated from a plasma torch to treat metal and organic contaminated wastes. This is accomplished by melting metal-bearing solids and, in the process, thermally destroying organic contaminants. The major components of the process are the plasma torch, the primary chamber containing a rotating crucible, manual feeder, and an off-gas treatment system.

The process operates as follows. Material to be treated is placed in the rotating crucible before the start of testing. This material is used as a base to form the molten pool. The plasma arc is initiated on a conductive water-cooled copper nose cone, which is centrally located at the bottom of the rotating crucible. Helium is used as the torch gas for torch ignition and nitrogen with 5% oxygen is used for operation. Oxygen is introduced through a separate port in sufficient amounts to produce an oxidizing atmosphere. The material adjacent to the copper nose cone is heated to conducting temperature first, then the torch is moved slowly outward to heat the remaining material in the rotating crucible. This creates a

molten pool at a temperature of 2500°F to 3000°F which is ready to receive the process material input. Additional material is fed manually through the feeder port. Solid material is retained in the crucible by centrifugal force while the plasma arc provides the heat to maintain the molten pool temperature as the material is reacted. At these temperatures, any organic contamination is volatilized from the material. Upon destruction of the organics and complete melting of the inert materials, the furnace is shut down, cooled, and the slag is manually removed. After removal, the slag is sampled for analysis and containerized.

The process off-gas is drawn off and passed through the off-gas treatment system. First, the off-gas is quenched, then passed through a packed bed to scrub out acidic gases and particulate. Process heat is removed from the off-gas and the temperature reduced to below 100°F. An air eductor?, located in the stack, promotes the flow of off-gas in the system and maintains the primary chamber at a slightly negative pressure.

Fe(II)/Fe(III) Ratio Analysis of Slags

Because the redox states of the elements in the slag affect its durability, the Fe(II)/Fe(III) ratios of selected glassy slags were analyzed. The Fe(II) content was obtained by first dissolving the slag in a hot, oxygen-free H_2SO_4 -HF solution, then immediately titrating the resulting solution with standardized $K_2Cr_2O_7$ solution. When two samples of standard Mohr salt $[Fe(NH_4)_2(SO_4)_2 \cdot 6H_2O]$ were treated in the same way, the recovery of Fe(II) was found to be 99.37% and 99.2%. The total Fe was measured by means of the Parr bomb and hot plate digestion process. The Fe(III) content was calculated as the difference of the Fe(II) and total Fe values obtained by the methods just described. The Fe(II)/Fe(III) ratios for the crucible slags are 0.40, 0.21, 0.36, 0.39, 0.34, 0.36, and 0.32 for ANL-M1, ANL-M4, ANL-M7, ANL-M8, ANL-M10, ANL-M11, and ANL-M12, respectively. The

Fe(II)/Fe(III) ratios for four PCF glassy slags [5] produced in the PCF are 1.69, 1.63, 1.59, and 0.924 for 92-BWID-2 (sample #1), 92-BWID-2 (sample #2), 93-BWID-1, and 93-BWID-3, respectively. These results indicate that the PCF produces more reduced slags (i.e., the metal oxides in the PCF slags are at lower oxidation states) than the crucible melts.

Durability Tests

The measure of the chemical durability of a glassy slag is its ability to resist corrosion when in contact with an aqueous solution or water vapor. The durability of the slags was determined by a modified Product Consistency Test (PCT) and by ANL vapor hydration tests.

Product Consistency Test

A static powder test similar to the PCT [6] was used to evaluate the relative durability of the glassy slags by measuring the concentrations of the elements released from the crushed glassy slags (75-150 μm) to the solution at 90°C. These tests were performed in deionized water in Teflon vessels. The ratio of the surface area of the slag to the volume of leachant (SA/V) was 2000 m^{-1} .

Vapor Hydration Test

The ANL vapor hydration test [7,8] was used as an accelerated corrosion test to measure the long-term durability of the glassy slags. This test is performed in saturated water vapor at 200°C. Durability is measured by the rate of formation of secondary alteration phases on the surface of the glassy slags, and the thickness of the altered surface layers on the samples was measured in cross section. This information provides insight into the long-

the samples was measured in cross section. This information provides insight into the long-term durability of glassy slags and provides another measure of the durability of high-level nuclear waste glasses.

Solution Analyses

Cations and radionuclides were analyzed with inductively coupled plasma - mass spectroscopy (ICP-MS) with an accuracy of $\pm 10\%$ for major elements and $\pm 50\%$ for radionuclides and minor elements. Anions were analyzed with ion chromatography with an accuracy of about 50%. The pH was analyzed with a pH meter with an accuracy of ± 0.1 pH unit.

Solids Analyses

The as-melted slags were analyzed by two methods: scanning electron microscopy (SEM) and transmission electron microscopy (TEM).

In the SEM analysis, spectra and images for both as-melted and reacted slags were collected on a Topcon ABT 60 SEM with a Princeton Gamma-Tech or Noran energy dispersive X-ray spectroscopy (EDS) system. The samples from the PCT tests were prepared by embedding many slag chips in a room-temperature-curing epoxy, then ground in cross section to a 600-grit finish, followed by a final polishing of 0.3 μm alumina. Monoliths from the vapor hydration tests were either mounted directly on an aluminum mounting stub and examined in the SEM or mounted in epoxy and cross-sectioned for layer thickness measurements.

In the TEM analysis, the reacted glassy slags were examined using a JEOL 2000FXII TEM operated at 200 kV and equipped with two EDS detectors and an electron

energy loss spectrometer (EELS). One EDS detector is an ultrathin-window (UTW) detector used for analyzing light elements. The other is a Be window detector that cannot detect elements below Na. Particles of slag were embedded in epoxy and sectioned by an ultramicrotome. EELS and a technique known as second difference analysis were used to improve the sensitivity for detecting cerium. In this technique, three spectra are obtained at increasing energy offset, which effectively removes the channel-to-channel gain variation. The structure of observed crystalline phases was determined by electron diffraction using the TEM with a double-tilt stage to obtain the zone axis pattern.

RESULTS AND DISCUSSION

Comparison of Crucible Slags and PCF Slags

Comparison of Formulations

The compositions of the eight slags recommended to MSE and the corresponding ANL melts are shown in Table 2. The eight slags were made by MSE in a 1.5-ft Retech PCF using carbon steel, stainless steel, INEL soil, and other metals and metal oxides. The actual metal loadings in the product were higher than those indicated in Table 2: as-received soil was used for formulations, and ~22% of the soil weight (mostly water) was lost during melting. These formulations were designed to achieve high loadings of Fe, Ni, and Cr (representing carbon steel and stainless steel) in slags, yet still produce a durable and processible product. A slight difference in the composition of final products between crucible and PCF slags was expected because of the differences in redox states of the metals and in

the contents of volatile metals of the resulting slags. In addition, slag properties may also be influenced by the processing environment.

Comparison of the As-Melted Slags

Five PCF slags, referred to as MAWS-1, MAWS-2, MAWS-4, MAWS-5, and MAWS-8, were received from MSE. They were characterized and compared to the slags produced in crucible melts at ANL. The general appearance of the slags produced in the ANL crucibles and in the 1.5-ft Retech PCF was similar. Three of the PCF slags were examined with SEM/EDS, and the results are summarized below.

MAWS-1. The sample appeared to contain glass and only one kind of crystal, on the basis of EDS analysis. The crystals near the sample surface are smaller than the particles in the sample center, but their compositions were similar (Fig. 1). The interface between the fine and coarse crystals was quite abrupt (Fig. 1a). The fine crystals are also shown in Fig. 1b and the coarse crystals are shown in Fig. 1c. Figures 2 and 3 provide the EDS spectra and composition data on the glass phase of MAWS-1. The glass phase consisted mainly of Si, Al, and Fe, with lesser amounts of K and Ca, very small amounts of Ce, and negligible amounts of Cr and Ni. The composition of the crystal phase is shown in Fig. 4: Fe_2O_3 is the dominant oxide, at 74%; Cr_2O_3 and Al_2O_3 are present, at ~12% each; and trace amounts of NiO were detected.

MAWS-4. This sample was also similar to the crucible melt ANL-M4 in both the types of crystals present and the compositions of the glass and crystalline phases (Fig. 5). The MAWS-4 slag appeared to contain two types of crystals (Fig. 5a). Two types of crystals were also observed in the corresponding crucible melt ANL-M4, as shown in Figs. 5b and 5c. The larger crystals in MAWS-4 were elongated, and the edge part of the large crystals

displayed contrast in backscattered imaging. The EDS composition of the center part of the larger crystals of MAWS-4 is shown in Fig. 6a; the crystals contained mainly Fe and Al, with small amounts of Cr and Ni. The EDS composition of the edge of the crystals that displayed contrast in backscattered imaging is shown in Fig. 7; the contrast may be due to the enrichment in chromium. The EDS spectrum (Fig. 6b) of crystals in ANL-M4 indicates that its composition is similar to that of MAWS-4. The glass phase contained many light gray fine crystals that were so small that their composition could not be determined with EDS.

Figure 8 represents the EDS composition of the region comprised of glass phase and the fine crystals.

MAWS-5. This sample showed that the metal was not fully oxidized during PCF processing. One of the examined samples contained several metallic inclusions that were probably stainless steel (Fig. 9a) because they were found to contain Fe, Ni, and Cr, with very little oxygen (Fig. 10). Also, a green band was visible in the optical microscope (Fig. 9b). This band appears bright in backscattered electron imaging and was richer in iron than the surrounding glass matrix (Fig. 11). Interestingly, the green band region did not contain crystallites, but it obviously contained more oxygen than the metal inclusion (compare Fig. 10 and Fig. 11), suggesting the iron may be mainly in a lower oxidation state; i.e., the carbon steel has not been fully oxidized to the higher oxidation state at which crystallinity would be expected. The majority of the MAWS-5 slag (Fig. 12b), however, was similar to crucible melt ANL-M10 (Fig. 12a); both have similar glass and crystal phases. The glass phase of MAWS-5 exhibited contrast in backscattered imaging (Fig. 9b), suggesting the presence of very fine crystallites rich in alumina (Fig. 13), which would result in an overestimation in the amount of aluminum in the glass. Another possible cause of the contrast differences is compositional variations; however, no compositional differences within

the glass were observed. Trace amounts of cerium were detected in the glass (Fig. 14). The crystals in MAWS-5 usually contained Fe, Cr, Ni, and Al oxides (Fig. 15), as did the crystal phase of ANL-M10. The glass phase of ANL-M10 showed less alumina than MAWS-5.

Comparison of Chemical Durability

A comparison of PCT test results for slags produced in the ANL crucible melts with the results for the PCF slags produced by MSE at Retech provides information that can be used to evaluate how well the crucible melts replicate the durability of the PCF melts. The available results from 7-, 28-, and 91-day PCT tests with the ANL slags (designated ANL-M#) and those produced in the 1.5-ft Retech PCF (designated MAWS-#) are presented in Table 3 as normalized mass losses (NL) for individual elements. In Table 3, results for slags with similar proportions of starting materials (see Table 2) are grouped together.

NL(Si) values are considered to be the most representative indicator of the durability of the glassy portion of the slag waste form. These values are used for three reasons: (1) silicon is a major component of the glass portion of the waste, (2) silicon concentrations are relatively high in the leachant, and (3) accurate silicon concentrations can be readily determined by ICP-MS. The use of silicon has two major drawbacks, in that this element can be readily incorporated in both Fe-Si colloids and many of the alteration phases that form on the altered slag surface. However, the lack of significant alteration phase development on the 7- and 28-day slag samples and no significant colloids observed in the leachates under TEM suggests that silicon may be used as a reliable indicator of the extent of glass reaction in the present tests. This assumption may not be valid in the longer term tests, in which more extensive alteration phases are expected to develop.

The NL(Si) values presented in Table 3 generally show good correspondence between the ANL crucible and PCF slags. Values for NL(Si) from 7- and 28-day PCT tests generally vary by less than a factor of two between the two slag products. The largest difference was found between the 7-day results for ANL-M7 and MAWS-8 samples, where the NL(Si) values varied by slightly less than a factor of three, but the 28-day results showed a difference of only 36%. The 91-day results for all the corresponding pairs of slags showed a difference of less than 60% except for the pair of ANL-16 and MAWS-2, where a factor of difference of 2.4 was observed. However, the 7- and 28-day differences of NL(Si) between ANL-16 and MAWS-2 were less than 5 and 28% respectively. In view of the reproducibility of the type of test employed (PCT) and the uncertainties in slag formulations, a difference of factor of two to three is not considered to be significant, especially from an performance assessment point of view. Thus, the NL(Si) results indicate that the ANL crucible melts can simulate the product from the 1.5-ft Retech PCF.

Comparisons of NL(i) release patterns for the remaining elements are less consistent than these patterns for silicon. Aluminum, sodium, and potassium comprise approximately 2 to 8, 0.2 to 0.8, and 0.5 to 1.7 oxide wt %, respectively, of each of the slag compositions (Table 2). All of the Na and K and most of the Al are partitioned into the glassy portion of the slag, as determined by SEM/EDS examination. The relative concentrations of these elements in the glass phase should be substantially higher than the values just listed because Na, K, and, to a lesser extent, Al are excluded from the Fe-rich crystalline phases.

The correspondence between NL(Al), NL(Na), and NL(K) values is relatively good for the ANL-M4 and MAWS-4 pairs and ANL-M7-and MAWS-8 pairs; generally, they vary by less than a factor of three (Table 3). Release trends for the remaining three slag comparisons, however, show considerably more data scatter. For these three sets of slags,

NL(Al) values vary by a factor of two to seven, NL(Na) values by a factor of two to eight, and NL(K) values by a factor of two to fourteen. The interpretation of these results is complicated somewhat by the difficulty of analyzing for potassium with the ICP-MS and the sorption of all three elements in clays that form on the altered glass surface. Silicon thus appears to be the best indicator of the performance of the glassy portion of the slag waste form. Future results, from longer-term samples, will be used to evaluate the differences noted between the release rate of Si and that of Al, Na, and K.

Cerium served as an analogue for plutonium in these simulated slag waste forms because CeO_2 and PuO_2 chemistry have been found to be similar in high-temperature glass melts [9]. SEM/EDS examinations indicated that cerium was preferentially fractionated into the glass portion of the slag. NL(Ce) values also varied between the ANL and PCF slags. The ANL slags consistently had higher NL(Ce) values than the corresponding PCF slags. The 7-day NL(Ce)s of ANL-M5, ANL-M7, ANL-M10, and ANL-M16 are higher by factors of 8, 105, 6, and 15, respectively, than the values for the corresponding PCF slags. An examination of the 28-day NL(Ce) indicates that the differences between the crucible melts and PCF melts were greatly reduced to only a factor of 1.6, 3.9, 1.4, and 5.2, respectively. The 91-day differences were a factor of 0.59, 0.68, 0.19, and 0.62 respectively. These results suggest that the differences in NL(Ce) may disappear with longer test durations. While some variation in the NL(Ce) values is expected in these tests, because of the relatively low cerium concentrations in the formulations, the consistent differences of the NL(Ce) values between the crucible and PCF products suggest that the differences may have resulted from the differences in the processing techniques (that resulted in differences in temperature of melts, tendency to volatilize, cooling rate, etc.) that, in turn, caused differences in solution chemistry.

These differences may be reasonably explained by the difference in the redox state of the bulk slags and the leachate pH's between the crucible and PCF slags. The examination of the PCF slags revealed metallic inclusions. In addition, the analysis of the PCF slags showed that their Fe(II)/Fe(III) ratios are at least a factor of three higher than those of the ANL crucible slags. Thus, it seems likely that there was a higher proportion of Ce³⁺ in the PCF slags than in the crucible slags. The hydrolysis constant for Ce³⁺ is 1×10^{-5} [10], which is much larger than the constant for Ce⁴⁺, 1.9×10^{-15} , suggesting that Ce³⁺ is more soluble in water than Ce⁴⁺. Some studies [11] suggested that the contribution of Ce⁴⁺ to the total soluble cerium in an air-saturated water system is less than 10%. On the other hand, the total Ce³⁺ solubility and speciation are strong functions of solution pH, and the major species are carbonate complexes, produced between pH 7 and 9 [11]. Barr et al. [11] reported that the solubility of total Ce³⁺ increased 58% for a pH change from 7 to 8 and 70% for a pH change from 7 to 9. Therefore, the total solubility of cerium in an aqueous system is a complex function of both Eh and pH. The finding that PCF slags are more reducing (in lower redox state) suggests a higher cerium release, but the lower 7-day leachate pH of PCF slags (Table 3) suggests a lower solubility of Ce³⁺ compared to the crucible slags. The observation that the 7-day NL(Ce) is lower in PCF slags suggests that pH is a more dominant factor in determining total cerium solubility. This may be consistent with the conclusion drawn by Baar et al. that the solubility of cerium in seawater is largely a function of pH rather than Eh [11]. Our PCT test condition is similar to a seawater system because the system is open to the oxygen and CO₂ in the atmosphere and the solution has a high salt content as a result of leaching. As the test duration increases, more and more of the Ce³⁺ on the surface of PCF slags is gradually converted to Ce⁴⁺, which will reduce the cerium solubility differences between the PCF and crucible slags for the longer test times. The solution pH trend of the

PCT test also increased as the test duration increased from 7 to 28 days (Table 3). This may explain why decreased differences in NL(Ce) between the crucible and PCF slags were observed for 28-day PCT tests. If this explanation holds, the NL(Ce) differences between crucible and PCF slags should be even smaller for the 91-day PCT tests and these were indeed observed in Table 3.

Comparisons of NL(Cr), NL(Ni), and NL(Fe) values from the crucible and PCF slags indicate a considerable amount of data scatter. Most of this variation can be attributed to analytical uncertainties related to accurately detecting the relatively low concentrations of these elements in solution. These low concentrations are a result of the relatively low solubilities of these elements in the leachates. Results from longer term tests will probably not provide any improved data, because the solution concentrations of these elements will probably remain low as a result of their incorporation into clay minerals on the reacted slag surfaces. Some insight into the performance of the crystalline phases and the behavior of Cr, Ni, and Fe may be gained in solid phase examinations of the reacted slag samples that will be conducted in the future.

CONCLUSIONS

Slag compositions developed through crucible melts were also successfully produced by MSE in a Retech PCF at Ukiah, California. The Retech tests were the initial feasibility studies on conducting the process in semicontinuous bench-scale equipment. The glassy slags produced at ANL were generally found to be similar to the slags produced in the PCF. The laboratory crucible melts produced glass and crystalline phases similar to those in the PCF slags and they exhibited similar chemical durability in terms of normalized release rates of the

major components of the slags, especially from a performance assessment point of view. Although the slags produced in the PCF using metals were usually less oxidized, this difference was found to have little effect on the corrosion behavior of the major components of the slags. A difference was observed in the normalized release of cerium between crucible slags and PCF slags, but this difference was decreased over time. The superior chemical durability and processibility of glassy slags will enable the MAWS approach to be applied to a much wider range of mixed wastes.

ACKNOWLEDGMENTS

This work is supported by the Office of Technology Development, within the U.S. Department of Energy's Office of Environmental Management, under Contract W-31-109-ENG-38 and DE-AC22-88ID12735. Special thanks are due to Roberta T. Riel for preparing this manuscript.

REFERENCES

1. I. L. Pegg, "Development of the Minimum Additive Waste Stabilization (MAWS) Program for Fernald," *Ceram. Trans.* 39, 13-22 (1994).
2. X. Feng, G. Ordaz, and P. Krumrine, "Glassy Slag - A Complementary Waste Form to Homogenous Glass for the Implementation of MAWS in Treating DOE Low-Level/Mixed Wastes," *Proc. Spectrum '94*, August 14-18, 1994, Atlanta, Georgia.
3. X. Feng, D. J. Wronkiewicz, J. K. Bates, N. R. Brown, M. Gong, and W. L. Ebert, "Glassy Slags as Novel Waste Forms for Remediating Mixed Wastes with High Metal Contents," *Proc. Waste Management '94*, February 27-March 4, 1994, Tucson, Arizona.
4. X. Feng et al., "Glassy Slags for Minimum Additive Waste Stabilization, Interim Progress Report, May 1993-February 1994," Argonne National Laboratory Report ANL-94/24 (1994).
5. S. T. Kujawa and C. W. Whiteworth, *Plasma Centrifugal Furnace Development Program at the CDIF*, Report No. 2DOE-PAFE-D010, MSE, Inc., Butte, MN (1993).
6. C. M. Jantzen, N. E. Bibler, D. C. Beam, W. R. Ramsey, and B. J. Waters, *Nuclear Waste Glass Product Consistency Test (PCT), Version 5.0*, Westinghouse Savannah River Co. Report WSRC-TR-90-539, Rev. 2 (1992).
7. J. K. Bates, L. J. Jardine, and M. J. Steindler, *The Hydration Process of Nuclear Waste Glass: An Interim Report*, Argonne National Laboratory Report ANL-82-11, pg. 32 (1982).
8. W. L. Ebert, J. K. Bates, and W. L. Bourcier, "The Hydration of Borosilicate Waste Glasses in Liquid Water and Steam at 200°C," *Waste Mgmt.* 11, 205-221 (1991).
9. R. E. McAtee and M. Beal, *Comparison of the High Temperature Chemistry of Plutonium and Rare Earths, A Review Study*, Idaho National Engineering Laboratory Report EGG-WTD-9801 (1991).
10. J. A. Dean, *Lange's Handbook of Chemistry*, 13th Ed., McGraw-Hill Book Company, New York, pp. 5-14 (1985).
11. H. Baar, J. W. De, C. R. German, H. Elderfield, and P. Van Gaans, "Rare Earth Element Distributions in Anoxic Waters of the Cariaco Trench," *Geochim. Cosmochim. Acta* 52, 1203-1219 (1988).

Table 1. Slag Compositions in Terms of Soil and Simulated Waste Metals, wt % As Mixed

ANL Slag	Carbon Steel	Stainless Steel	Soil	Aluminum	Lead	CeO ₂	Sand
ANL-M1	62.1		37.9				
ANL-M2	73.7		26.3				
ANL-M3		15.0	85.0				
ANL-M4		30.0	70.0				
ANL-M5	50.0		50.0			1.0	
ANL-M6	54.0		20.0	5.0		1.0	20.0
ANL-M7	47.0	24.0	28.0			1.0	
ANL-M8	39.9	17.1	34.9	4.7	2.0	1.1	
ANL-M9	40.0	15.0	45.0			1.0	
ANL-M10	45.0	10.0	44.0			1.0	
ANL-M11	43.0	10.0	44.0		2.0	1.0	
ANL-M12	45.0 (2% Cl)	10.0	44.0			1.0	
ANL-M13	47.0	8.0	44.0			1.0	
ANL-M14		10.0	89.0			1.0	
ANL-M15	49.0	10.0	38.0		2.0	1.0	
ANL-M16	69.0		30.0			1.0	

Table 2. Formulations Recommended to MSE, Inc., wt %

PCF Slag	Carbon Steel ^a	Stainless Steel ^b	Soil ^c	FeCl ₃	Lead	CeO ₂	Corresponding ANL Melt
MAWS-1	50		49			1	ANL-M5
MAWS-2	70		29			1	ANL-M16
MAWS-3		10	89			1	ANL-M14
MAWS-4		29	70			1	ANL-M4
MAWS-5	45	10	44			1	ANL-M10
MAWS-6	43	10	44		2	1	ANL-M11
MAWS-7	44	10	44	3		1	ANL-M12
MAWS-8	50	20	29			1	ANL-M7

^aCarbon steel = 99.8% Fe.^bStainless steel = 68.4% Fe, 19% Cr, and 9.3% Ni.^cINEL soil was used as received and the dried soil has 12.1% Al₂O₃, 0.1% BaO, 8.4% CaO, 5.4% Fe₂O₃, 2.5% K₂O, 2.4% MgO, 0.1% MnO₂, 1.2% Na₂O, 0.1% Sb₂O₃, 66.7% SiO₂, and 0.7% TiO₂.

Table 3. PCT Results for Crucible and PCF Slags, Normalized Release, g/m²

Slag	Reaction Days	pH	Al	Cr	Fe	K	Ce	Ni	Na	Si
ANL-M4	7	8.72	0.0247	0.000012	0.000413	0.0821	0.000055	0.1982	0.0467	
	28	8.29	0.0447	0.000018	0.000000	0.0732	0.000000	0.1957	0.0539	
	91	8.12	0.0429	0.000033	0.000098	0.0583	0.000031	0.1907	0.0551	
MAWS-4	7	7.85	0.0394	0.000131	0.000015	0.0255	0.000088	0.2001	0.0310	
	28	8.73	0.0447	0.000133	0.000045	0.0443	0.000031	0.2581	0.0427	
	91	7.97	0.0540	0.000150	0.000040	0.0792	0.000030	0.4108	0.0589	
ANL-M5	7	8.22	0.0461	0.000072	0.1387	0.000436	0.2591	0.0819		
	28	7.89	0.0866	0.000393	0.1402	0.000399	0.3092	0.0934		
	91	8.32	0.0929	0.000048	0.1319	0.000327	0.3141	0.0983		
MAWS-1	7	8.07	0.1207	0.000122	0.2633	0.000060	1.8066	0.0608		
	28	8.56	0.1649	0.000393	0.3433	0.000254	2.4404	0.0753		
	91	8.07	0.1587	0.000400	0.3675	0.000550	2.8772	0.0785		
ANL-M7	7	8.15	0.1755	0.000000	0.2619	0.000422	0.000079	0.5934	0.1610	
	28	7.76	0.1387	0.000064	0.2459	0.000683	0.000088	0.6277	0.1715	
	91	8.27	0.0919	0.000033	0.000075	0.2724	0.000724	0.6315	0.1653	
MAWS-8	7	7.33	0.0279	0.000002	0.000000	0.0187	0.000004	0.000148	0.2424	0.0561
	28	8.15	0.0570	0.000002	0.000009	0.0305	0.000173	0.000055	0.3389	0.1258
	91	7.40	0.0660	0.000002	0.000009	0.0821	0.001100	0.000055	0.6147	0.1578
ANL-M10	7	8.45	0.0542	0.000045	0.000086	0.1465	0.000254	0.000217	0.3199	0.1024
	28	7.79	0.0574	0.000060	0.000458	0.2440	0.000313	0.000352	0.5027	0.1464
	91	8.60	0.0604	0.000061	0.000051	0.1482	0.000149	0.000058	0.4059	0.1028
MAWS-5	7	8.13	0.1338	0.002588	0.000002	0.0332	0.000058	0.000037	0.9351	0.0624
	28	8.29	0.1365	0.002675	0.000025	0.0644	0.000229	0.000057	1.2255	0.0751
	91	7.87	0.1416	0.002200	0.000020	0.0895	0.000800	0.000100	1.5219	0.0827
ANL-M16	7	8.09	0.0915		0.000056	0.2626	0.000629		0.4373	0.1449
	28	7.00	0.0542		0.000100	0.4303	0.000411		0.7289	0.2481
	91	8.48	0.1008		0.000037	0.2319	0.000498		0.4685	0.1475
MAWS-2	7	7.39	0.2220		0.000061	0.1275	0.000043		1.7783	0.1528
	28	8.80	0.2828		0.000049	0.2352	0.000079		3.3504	0.1941
	91	8.83	0.1737		0.000300	0.3408	0.0008		4.8735	0.3663

Table 3. PCT Results for Crucible and PCF Slags, Normalized Release, g/m²

Slag	Reaction Days	pH	Al	Cr	Fe	K	Ce	Ni	Na	Si
ANL-M4	7	8.72	0.0247	0.000012	0.000413	0.0821		0.000055	0.1982	0.0467
	28	8.29	0.0447	0.000018	0.000000	0.0732		0.000000	0.1957	0.0539
	91	8.12	0.0429	0.000033	0.000098	0.0583		0.000031	0.1907	0.0551
MAWS-4	7	7.85	0.0394	0.000131	0.000015	0.0255		0.000088	0.2001	0.0310
	28	8.73	0.0447	0.000133	0.000045	0.0443		0.000031	0.2581	0.0427
	91	7.97	0.0540	0.000150	0.000040	0.0792		0.000030	0.4108	0.0589
ANL-M5	7	8.22	0.0461		0.000072	0.1387	0.000436		0.2591	0.0819
	28	7.89	0.0866		0.000393	0.1402	0.000399		0.3092	0.0934
	91	8.32	0.0929		0.000448	0.1319	0.000327		0.3141	0.0983
MAWS-1	7	8.07	0.1207		0.000122	0.2633	0.000060		1.8066	0.0608
	28	8.56	0.1649		0.000393	0.3433	0.000254		2.4404	0.0753
	91	8.07	0.1587		0.000400	0.3675	0.000550		2.8772	0.0785
ANL-M7	7	8.15	0.1155	0.000000	0.000083	0.2619	0.000422	0.000079	0.5934	0.1610
	28	7.76	0.1387	0.000064	0.000000	0.2459	0.000683	0.000088	0.6277	0.1715
	91	8.27	0.0919	0.000033	0.000075	0.2724	0.000724	0.000041	0.6315	0.1653
MAWS-8	7	7.33	0.0279	0.000002	0.000000	0.0187	0.000004	0.000148	0.2424	0.0561
	28	8.15	0.0570	0.000002	0.000009	0.0305	0.000173	0.000055	0.3389	0.1258
	91	7.40	0.0660	0.000002	0.000009	0.0821	0.001100	0.000055	0.6147	0.1578
ANL-M10	7	8.45	0.0542	0.000045	0.000086	0.1465	0.000354	0.000217	0.3199	0.1024
	28	7.79	0.0574	0.000060	0.000458	0.2440	0.000313	0.000352	0.5027	0.1464
	91	8.60	0.0604	0.000061	0.000051	0.1482	0.000149	0.000058	0.4059	0.1028
MAWS-5	7	8.13	0.1338	0.002588	0.000002	0.0332	0.000058	0.000037	0.9351	0.0624
	28	8.29	0.1365	0.002675	0.000025	0.0644	0.000229	0.000057	1.2255	0.0751
	91	7.87	0.1416	0.002200	0.000020	0.0895	0.000800	0.000100	1.5219	0.0827
ANL-M16	7	8.09	0.0915		0.000056	0.2626	0.000629		0.4373	0.1449
	28	7.00	0.0542		0.000100	0.4303	0.000411		0.7289	0.2481
	91	8.48	0.1008		0.000037	0.2319	0.000498		0.4685	0.1475
MAWS-2	7	7.39	0.2220		0.000061	0.1275	0.000043		1.7783	0.1528
	28	8.80	0.2828		0.000049	0.2352	0.000079		3.3504	0.1941
	91	8.83	0.1737		0.000300	0.3408	0.00008		4.8735	0.3663

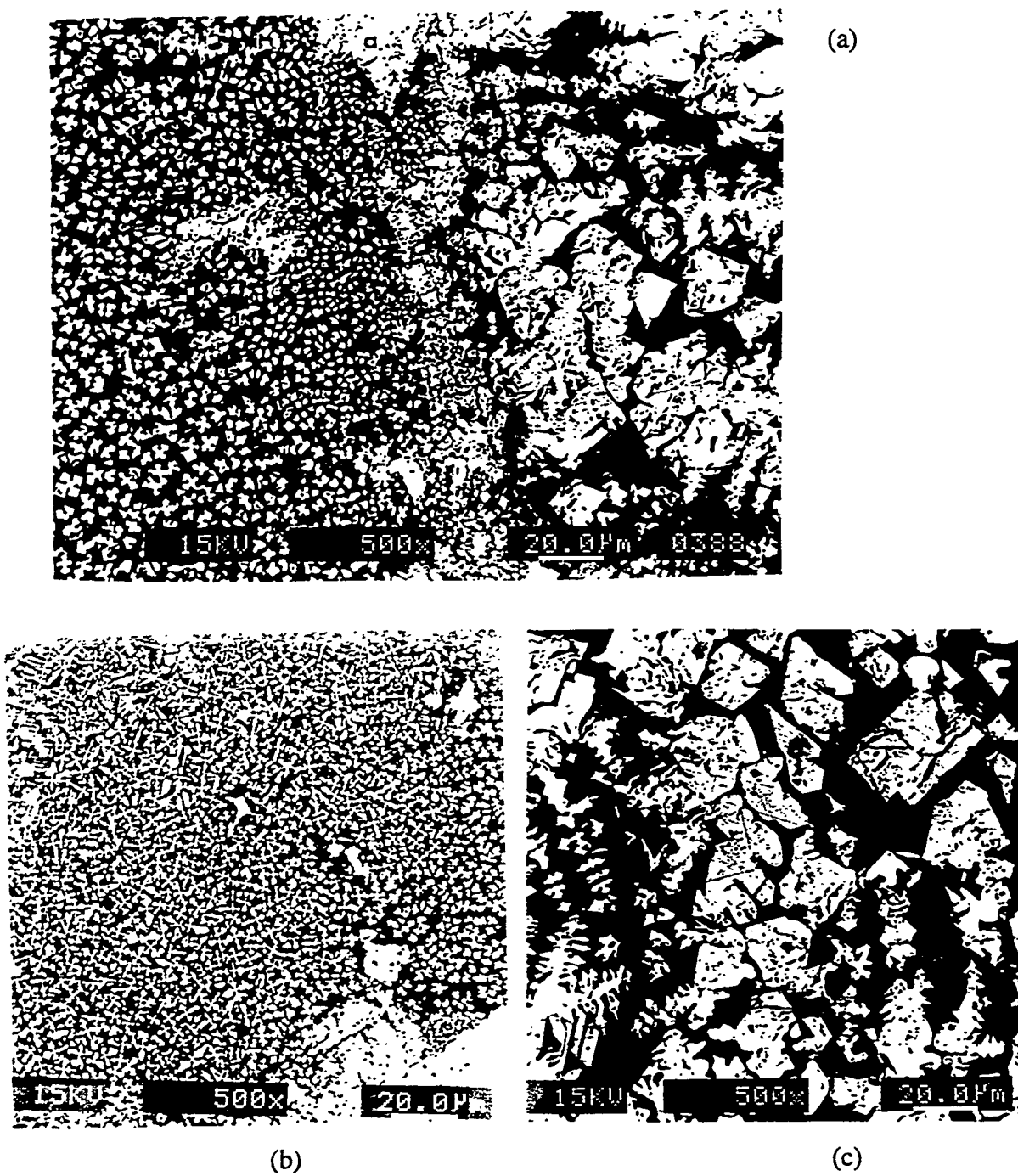


Fig. 1. SEM Micrographs of MAWS-1: (a) Both Fine and Coarse Crystals; (b) Fine Crystals Only; (c) Coarse Crystals Only.

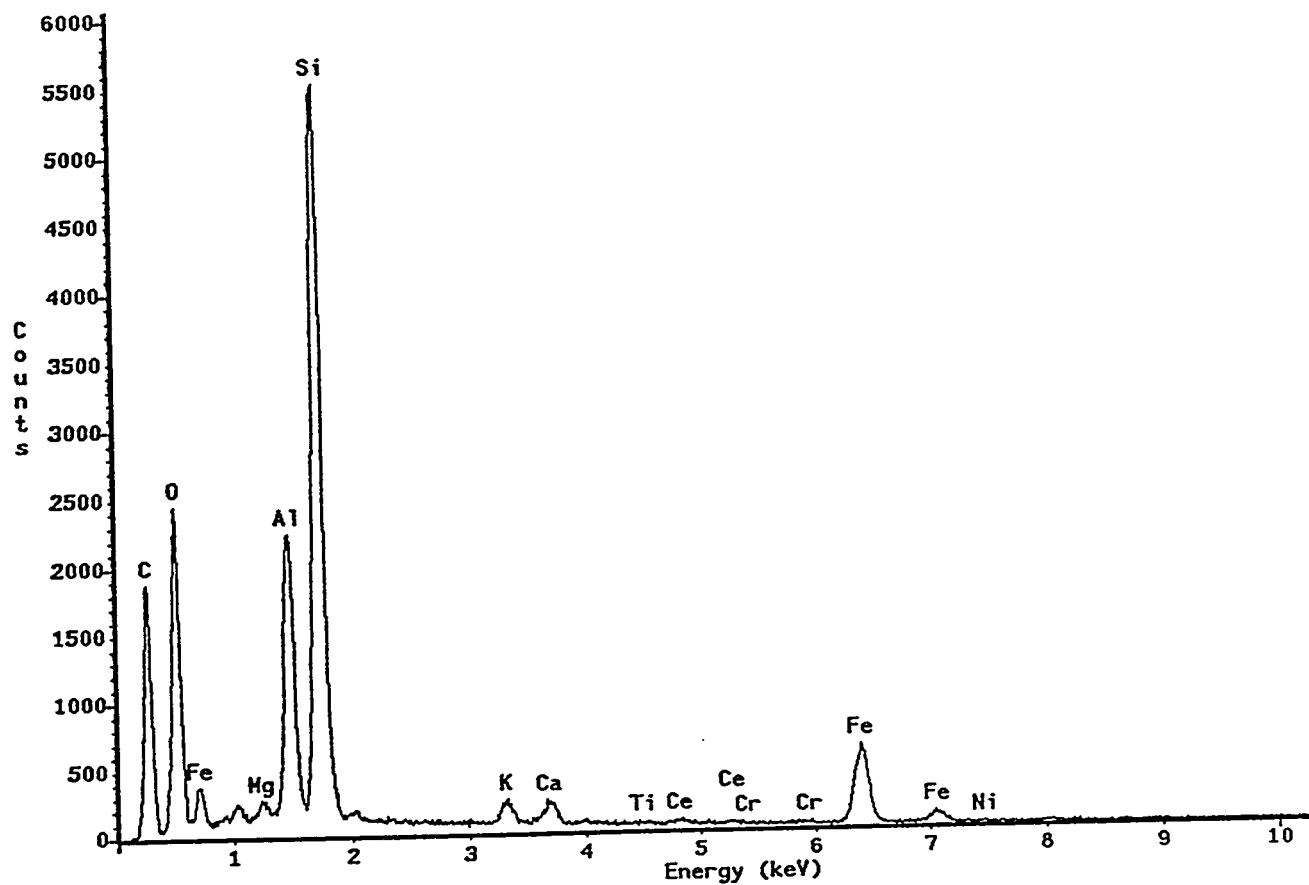


Fig. 2. EDS Spectrum of the Glass Phase in MAWS-1.

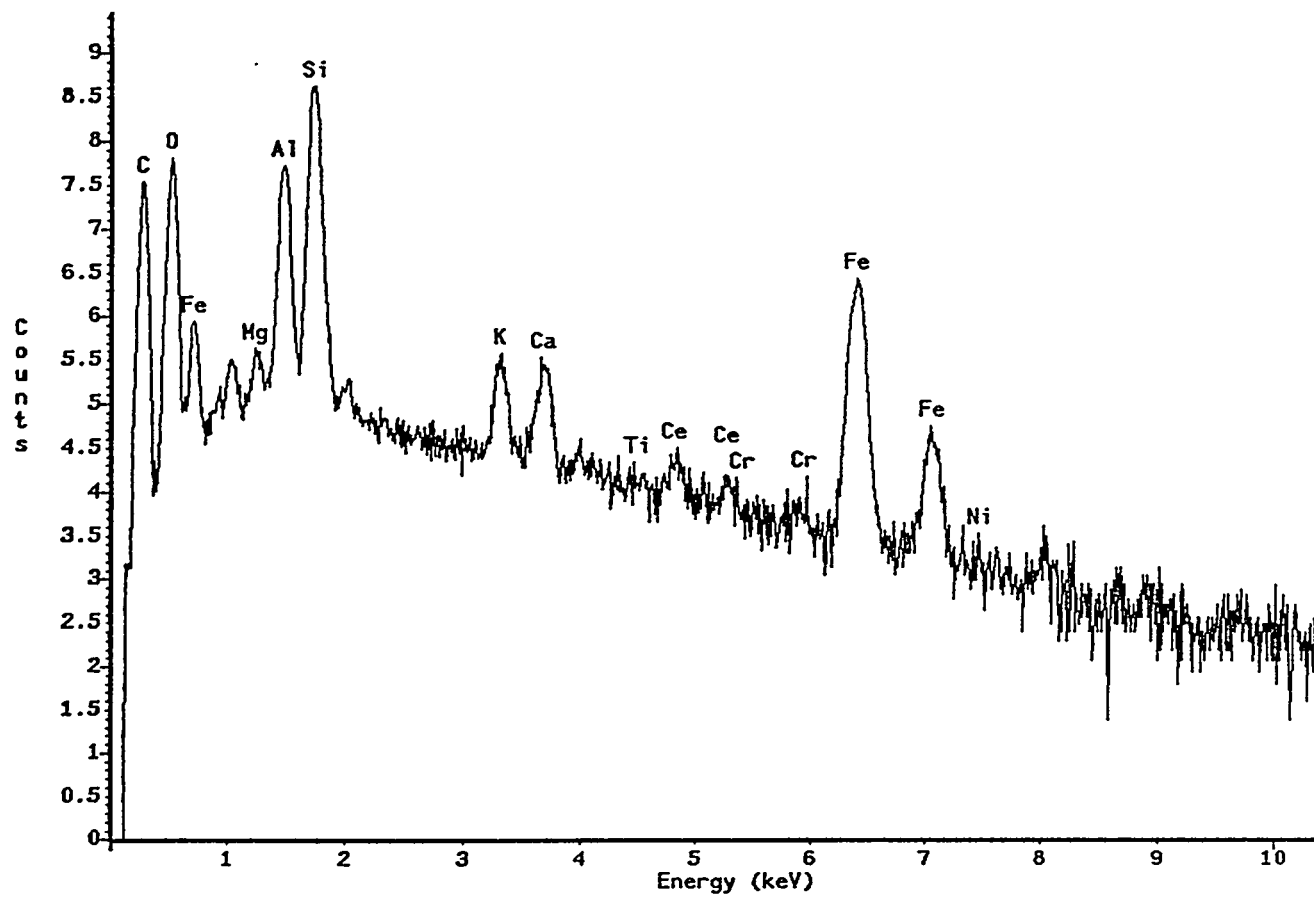


Fig. 3. EDS Spectrum of the Glass Phase in MAWS-1 with Vertical Axis in Log Scale.

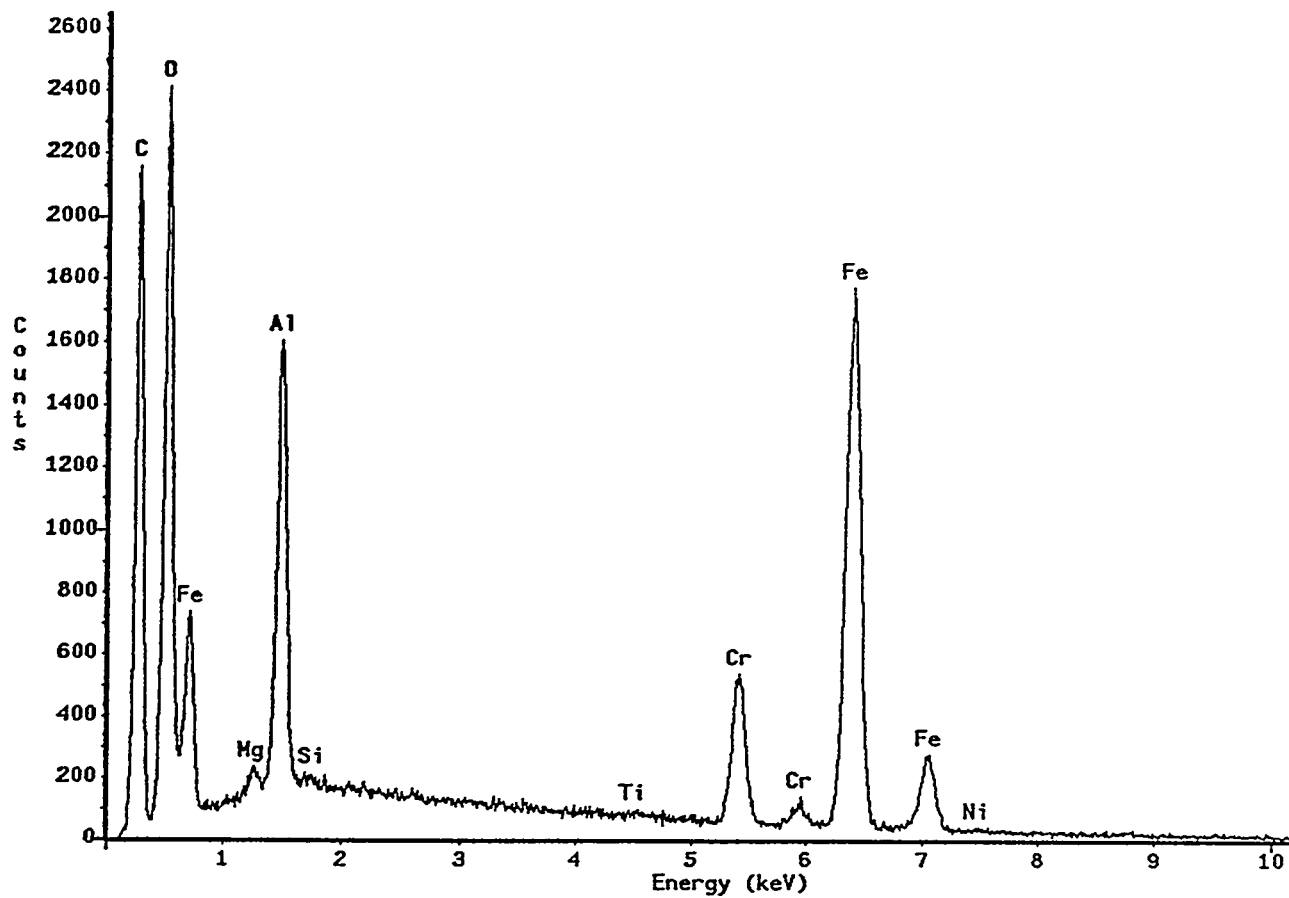


Fig. 4. EDS Spectrum of the Crystalline Phase in MAWS-1.

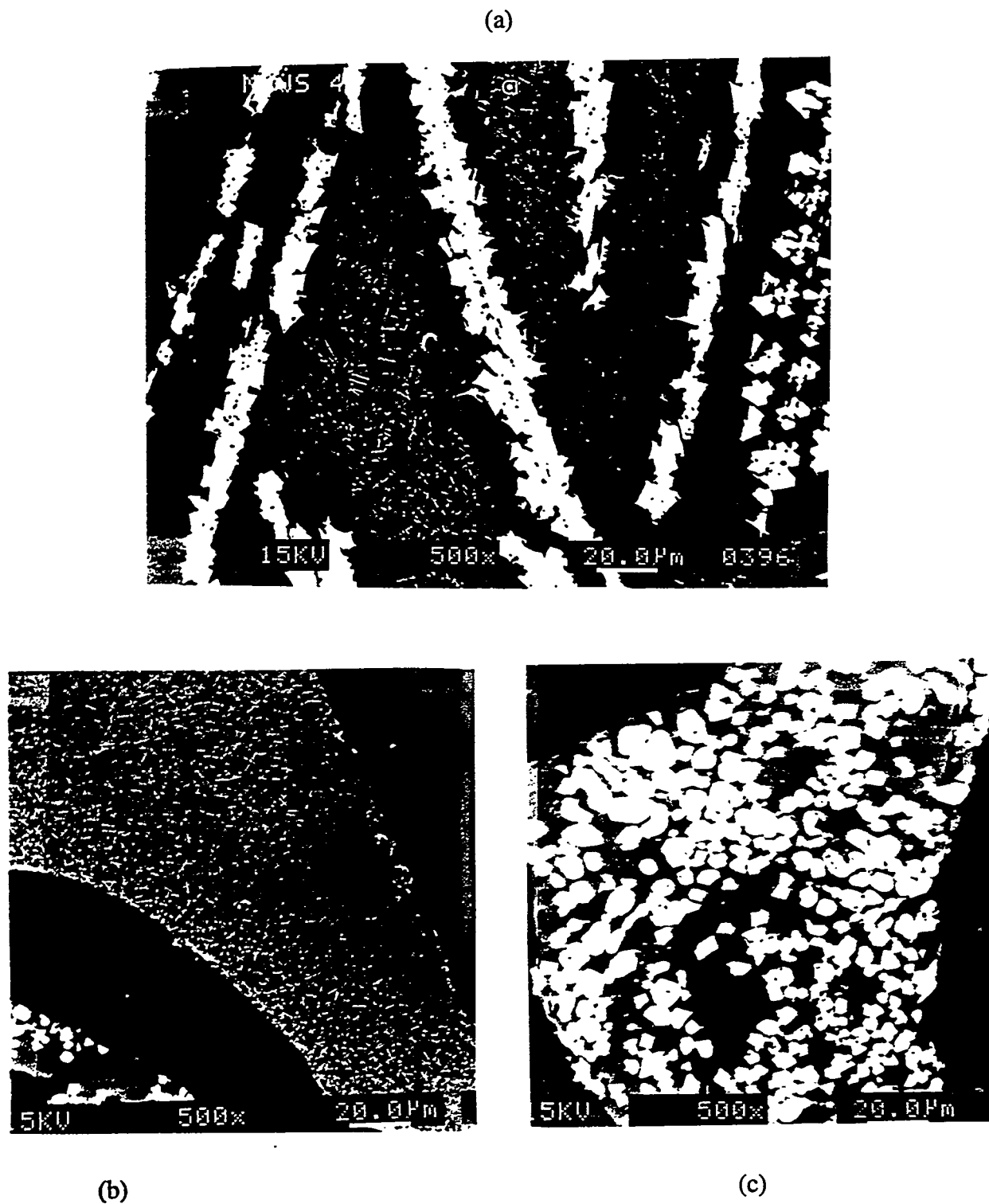


Fig. 5. SEM Micrographs of (a) MAWS-4, (b) ANL-M4 (5 kV), and (c) ANL-M4 (15 kV).

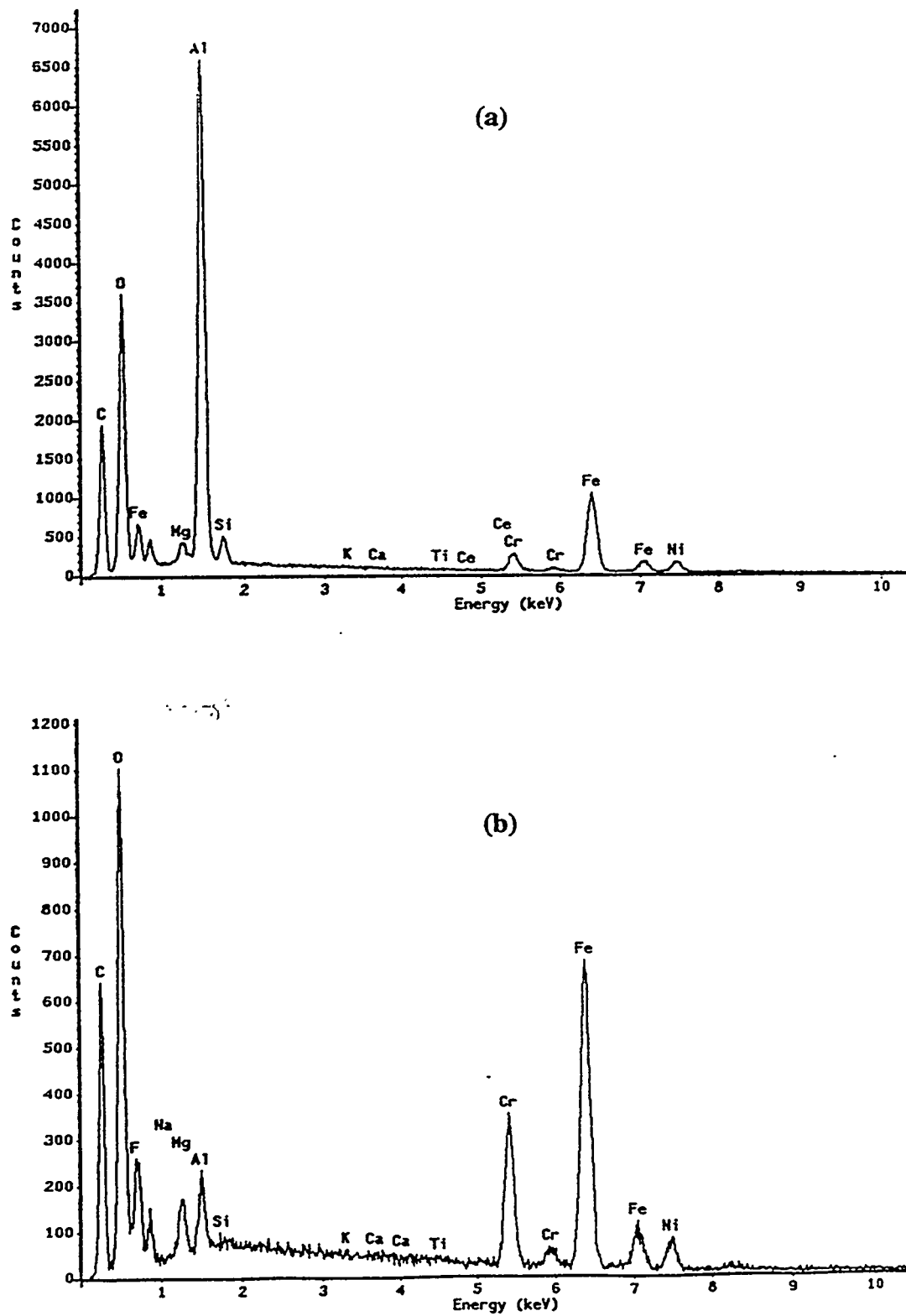


Fig. 6. EDS Spectrum of (a) the Larger Crystals in MAWS-4 and (b) the Crystals in ANL-M4.

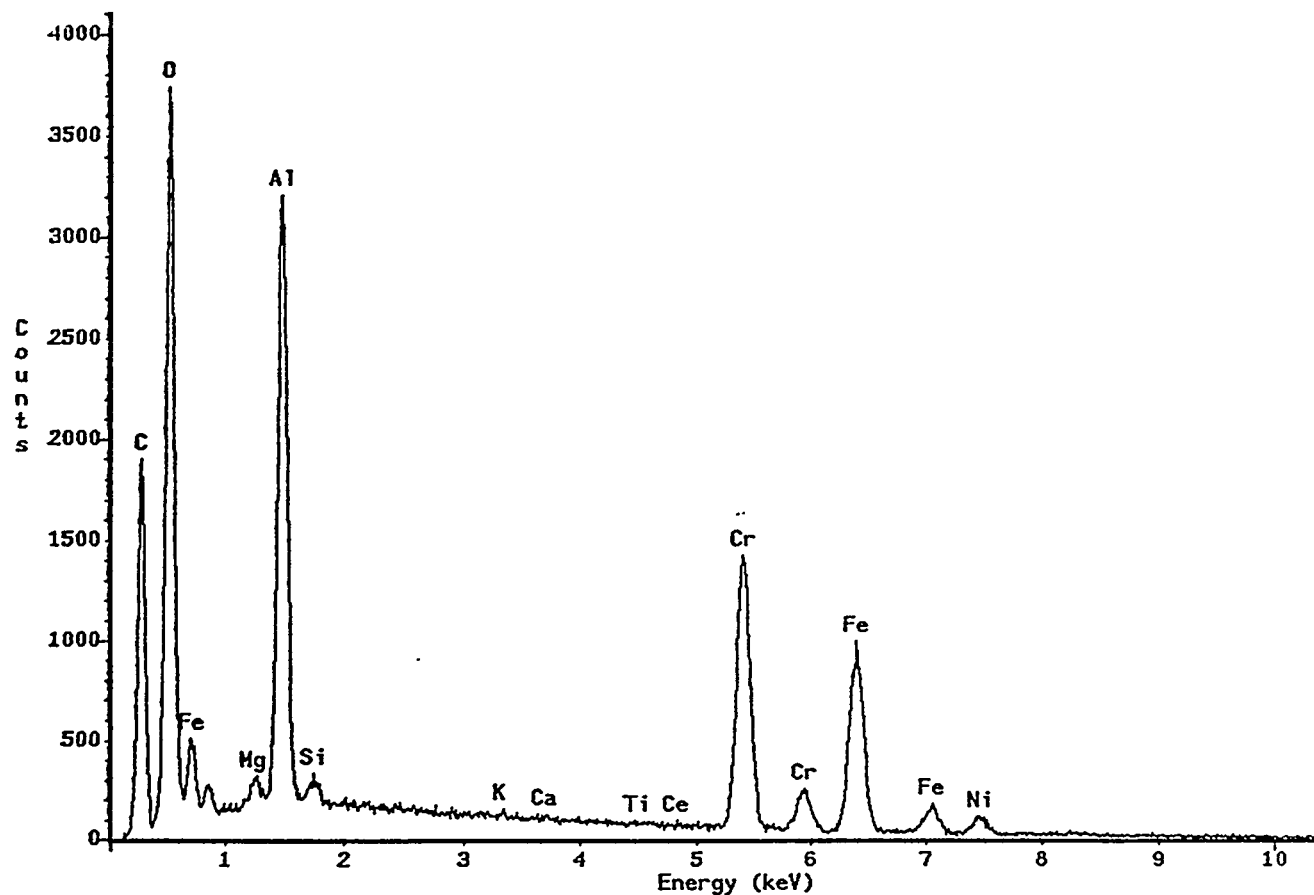


Fig. 7. EDS Spectrum of the Edge Part of the Large Crystals of MAWS-4 that Displayed Contrast in Backscattered Imaging.

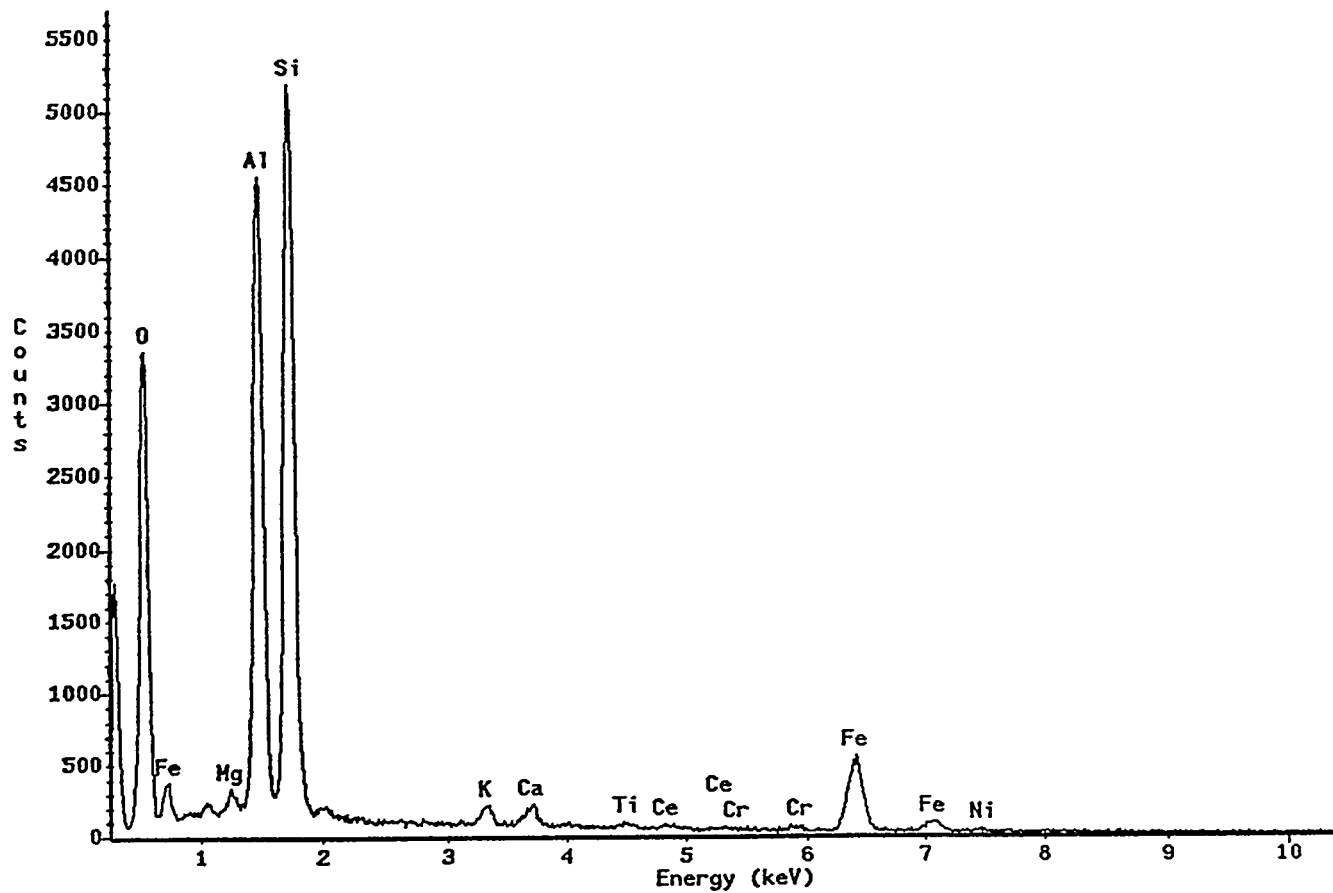


Fig. 8. EDS Spectrum of the Glass Phase (Including the Fine Crystals) in MAWS-4.

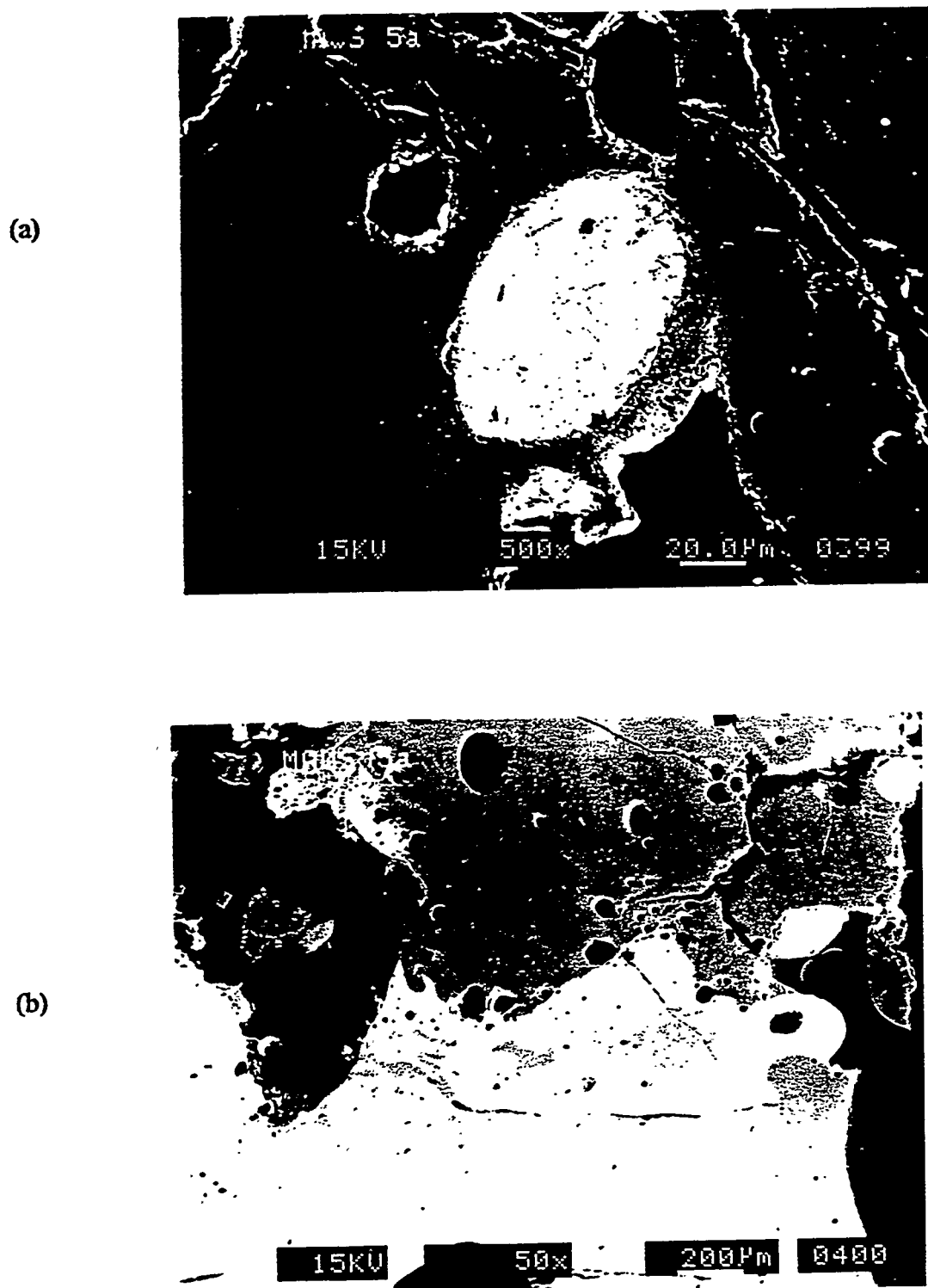


Fig. 9. SEM Micrographs of MAWS-5: (a) Metallic Inclusion and (b) Bright Band.

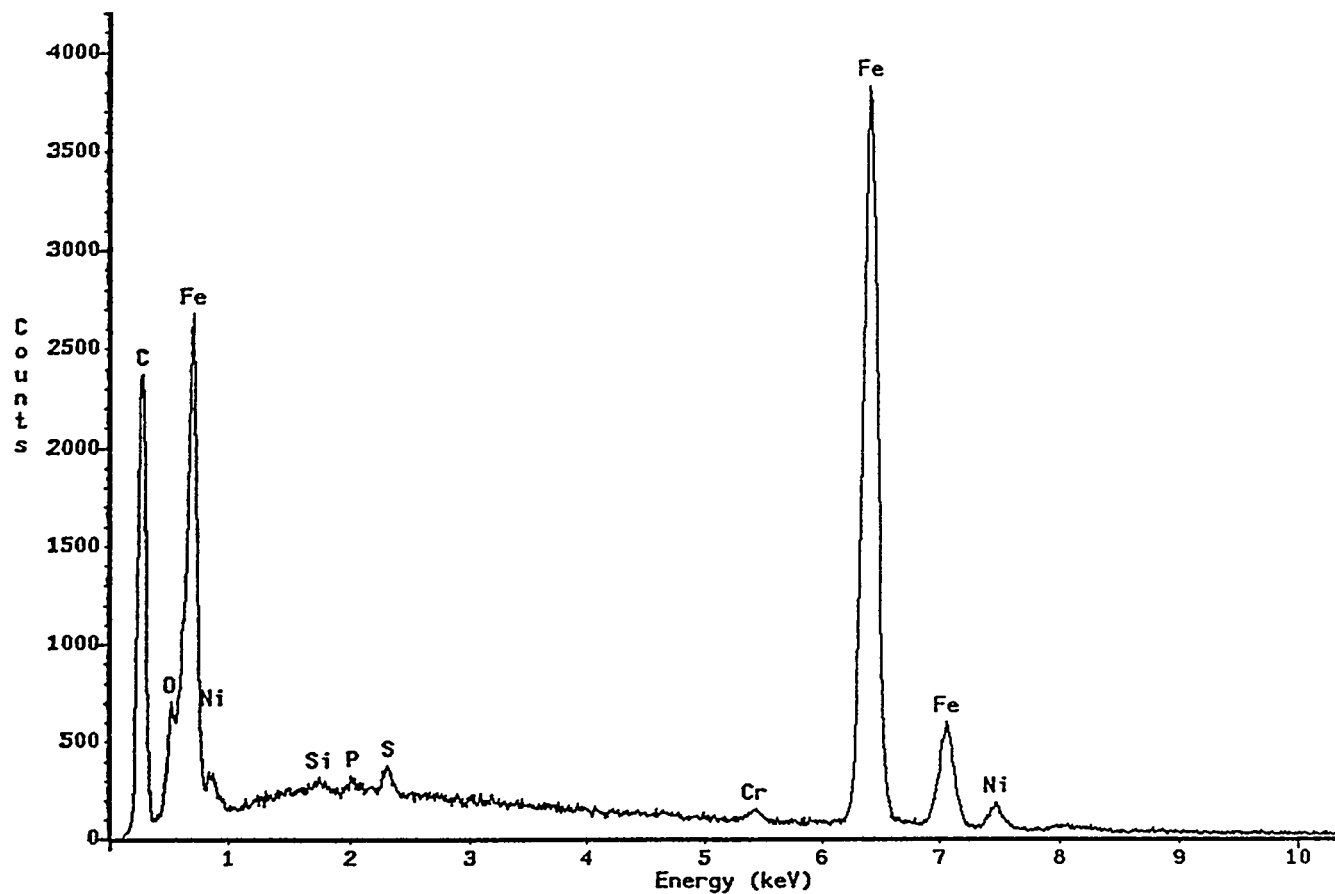


Fig. 10. EDS Spectrum of the Metallic Inclusion in MAWS-5.

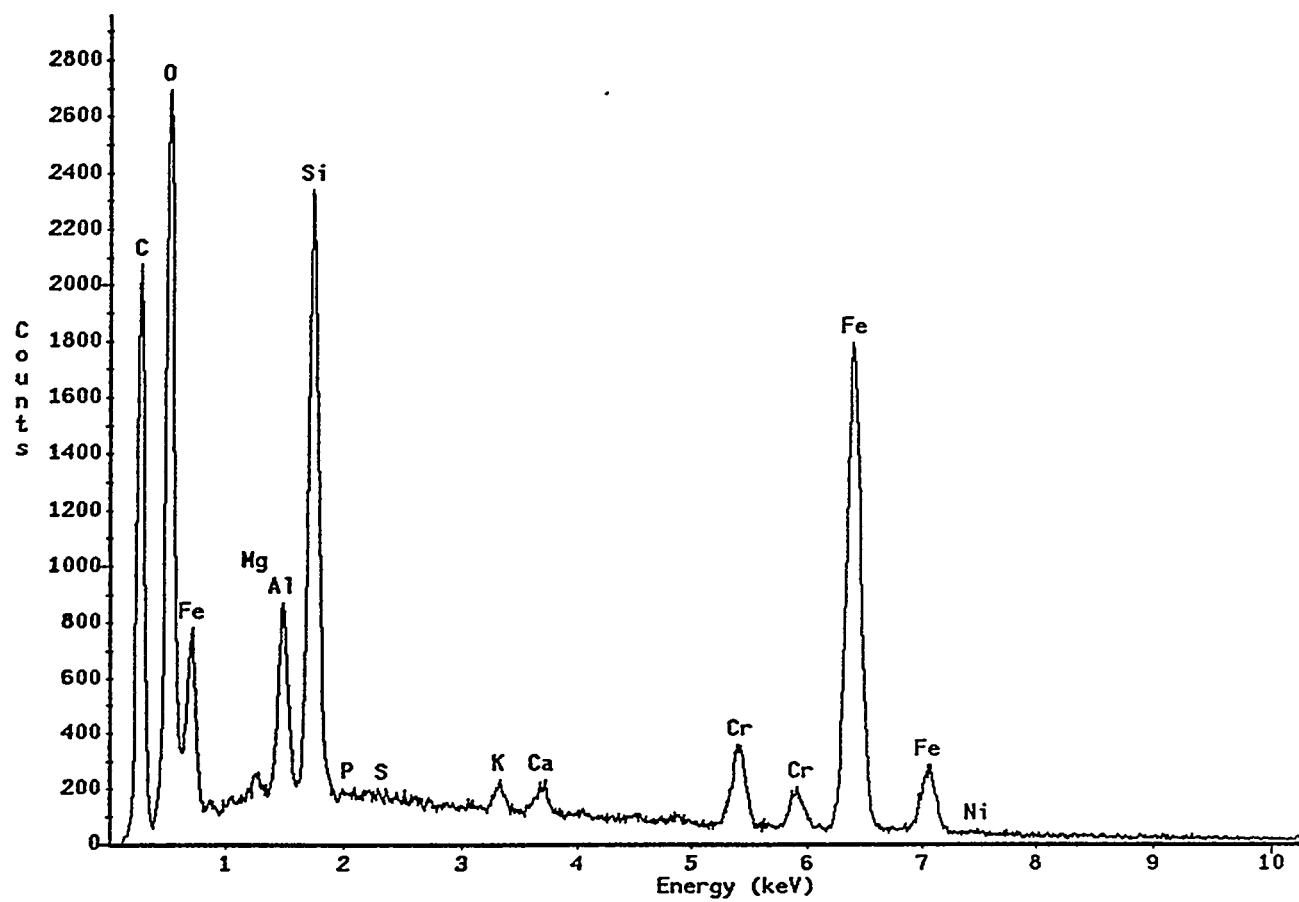
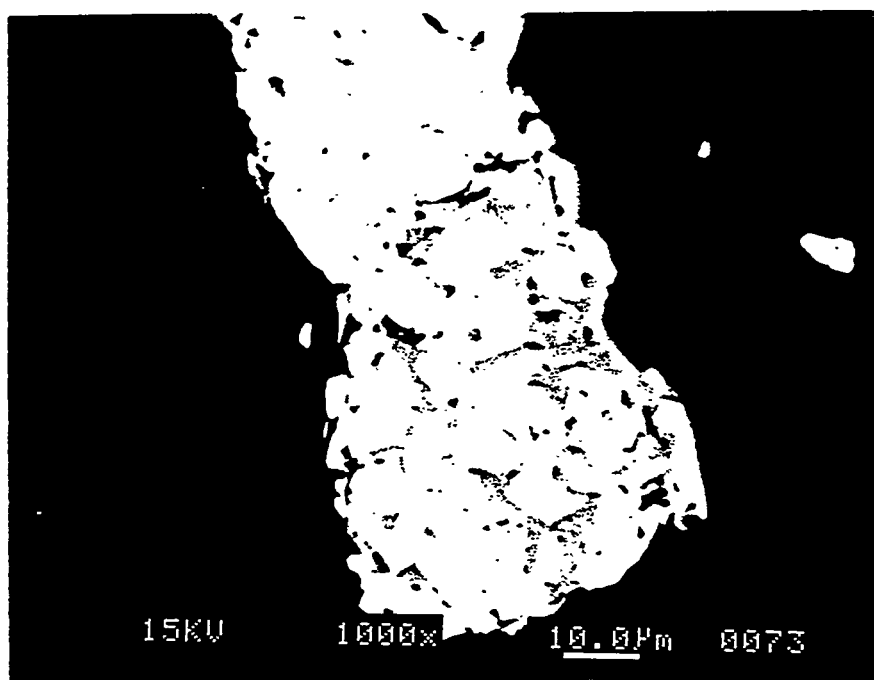


Fig. 11. EDS Spectrum of the Bright Band in MAWS-5.

(a)



(b)

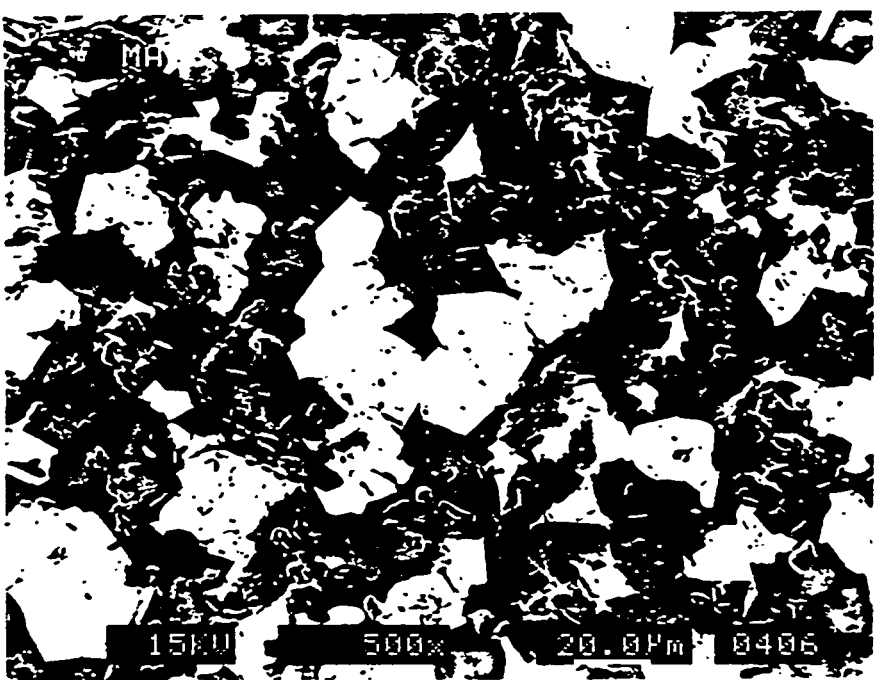


Fig. 12. SEM Micrographs of (a) ANL-M10 and (b) MAWS-5.

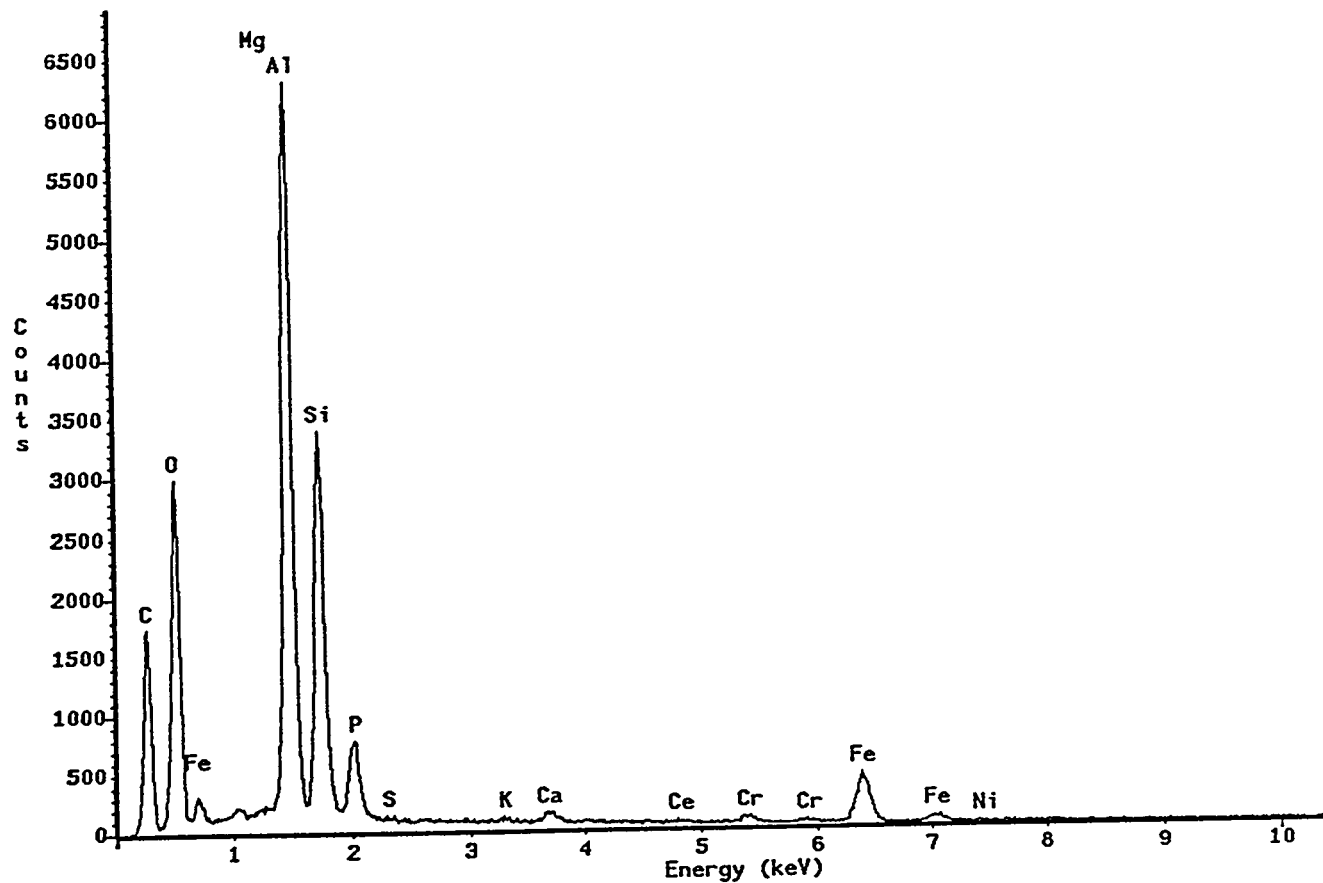


Fig. 13. EDS Spectrum of the Glass Phase with Fine Crystals in MAWS-5.

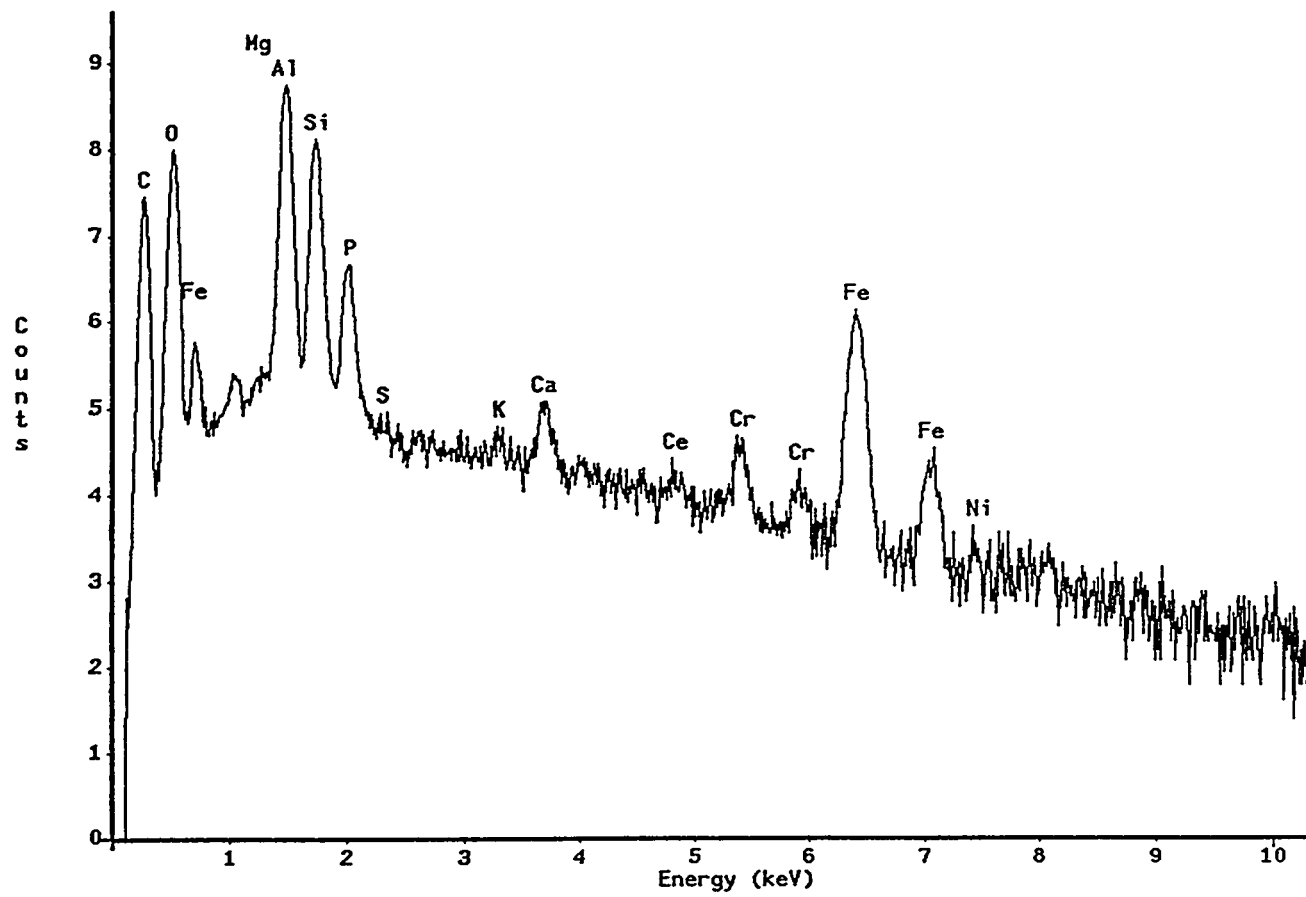


Fig. 14. EDS Spectrum of the Glass Phase with Fine Crystals in MAWS-5, with Vertical Axis in Log Scale.

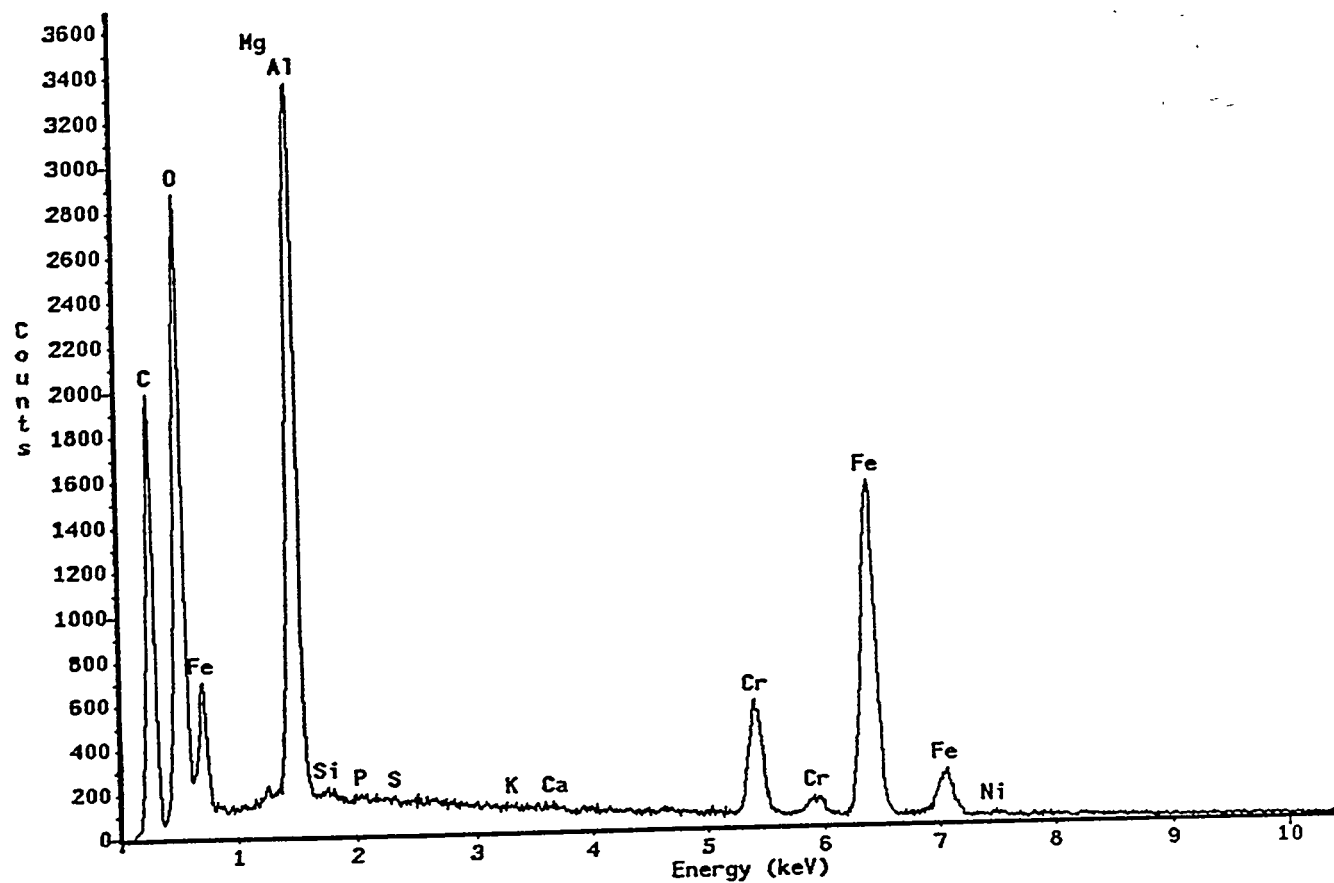


Fig. 15. EDS Spectrum of the Crystal Phase in MAWS-5.